



Published in final edited form as:

*ACS Chem Neurosci.* 2017 August 16; 8(8): 1779–1788. doi:10.1021/acscchemneuro.7b00148.

## Enhancing Continuous Online Microdialysis using Dexamethasone: Measurement of Dynamic Neurometabolic Changes during Spreading Depolarization

Erika L. Varner<sup>1</sup>, Chi Leng Leong<sup>2</sup>, Andrea Jaquins-Gerstl<sup>1</sup>, Kathryn M. Nesbitt<sup>1</sup>, Martyn G. Boutelle<sup>2</sup>, Adrian C. Michael<sup>1,\*</sup>

<sup>1</sup>Department of Chemistry, University of Pittsburgh, Pittsburgh, PA 15260, USA

<sup>2</sup>Department of Bioengineering, Imperial College London, London SW7 2AZ, UK

### Abstract

Microdialysis is well established in chemical neuroscience as a mainstay technology for real time intracranial chemical monitoring in both animal models and human patients. The capabilities of microdialysis sampling have the potential to be further enhanced through mitigation of the penetration injury unavoidably caused by the insertion of microdialysis probes into brain tissue. Herein, we show that dexamethasone retrodialysis in the rat cortex enhances the microdialysis detection of K<sup>+</sup> and glucose transients induced by spreading depolarization. Once inserted, the probes were perfused continuously (1.67 μL/min) either with or without dexamethasone. Without dexamethasone, glucose transients were too small to reliably quantify at 5 days after probe insertion. With dexamethasone, robust K<sup>+</sup> and glucose transients were readily quantified at 2 hrs, 5 days, and 10 days after probe insertion. Although the amplitudes of the K<sup>+</sup> transients declined day-to-day following probe insertion, amplitudes of the glucose transients were consistent. Immunohistochemistry and fluorescence microscopy confirm that dexamethasone is highly effective at preventing ischemia and gliosis in the vicinity of microdialysis probes implanted for 10 days.

### Graphical Abstract

\*Corresponding Author University of Pittsburgh, Dept. of Chemistry, 219 Parkman Ave., Pittsburgh, PA 15260, USA., amichael@pitt.edu. Phone: 412-624-8560.

#### Author Contributions

ELV, CLL, AJG, and KMN collaborated on the collection of microdialysis results. CLL set up the rsMD and K<sup>+</sup> detector systems in Pittsburgh and trained ELV and AJG in its use. AJG collected brain tissues, performed the immunohistochemical procedures, collected the microscope images, and quantitatively analyzed the images. All authors participated in the design of the experiments, evaluation of the results, and preparation of the manuscript.

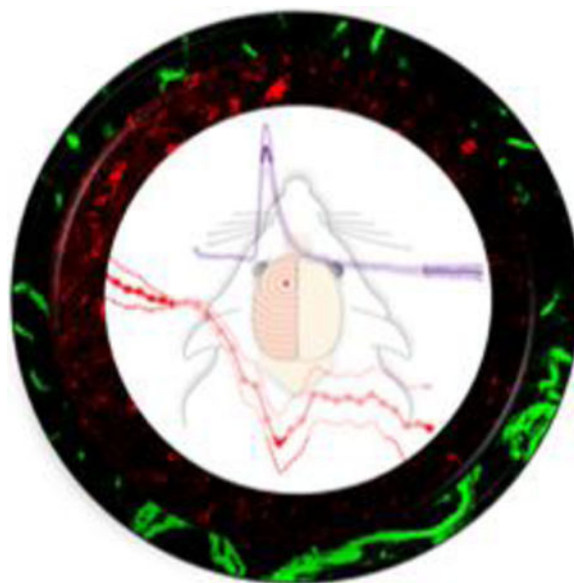
#### ASSOCIATED CONTENT

##### Supporting Information

Additional information as noted in text (Supporting Figures S1–S4 and Table S1). This material is available free of charge via the Internet at <http://pubs.acs.org>.

#### Conflict of Interest

The authors declare no competing financial interest.



## Keywords

Microdialysis; dexamethasone; biosensor; microfluidic; spreading depolarization

The high incidence of traumatic brain injury (TBI) is a significant health crisis, described recently as a 'silent epidemic'.<sup>1,2</sup> In the United States, 1.7 million brain injuries per year lead to 275,000 hospitalizations and 52,000 deaths.<sup>3</sup> The heart of the problem is secondary brain injury, which can cause death many days after the primary TBI even though the patient is under intensive care. Secondary injury occurs when the so-called penumbra is subjected to secondary insults, such as rises in intracranial pressure, transient ischemia, seizures, and spreading depolarization (SD). Neuromonitoring after severe TBI detects SD<sup>4-9</sup> in approximately 60% of patients.<sup>10-13</sup> SD is a pathological mechanism for secondary injury that drives expansion of the brain lesion into the penumbra.<sup>9-15</sup> Incidence of SD is significantly correlated with poor patient outcomes, including death, vegetative state, and severe disability.<sup>7-9</sup> SD disrupts the concentration gradients of ions and molecules between intra- and extracellular spaces, and repolarization after SD requires vast amounts of energy.<sup>7-9</sup> Clusters of SD impose particularly severe energy demands on the injured brain.<sup>15-18</sup>

Clinical microdialysis facilitates monitoring of the local metabolic status of brain tissue in patients with TBI.<sup>18-24</sup> Boutelle and coworkers developed a rapid sampling microdialysis (rsMD) system that monitors glucose with 30-s temporal resolution.<sup>19</sup> By the combination of rsMD with an online ion selective electrode (ISE), simultaneous rapid monitoring of glucose and  $K^+$  is now possible.<sup>21, 24-25</sup>

Microdialysis is well-established for real time intracranial chemical monitoring.<sup>26-27</sup> Nevertheless, inserting the probe into brain tissue causes a penetration injury.<sup>28-35</sup> In response, the host tissue engulfs the probe in a glial barrier that, once formed, impairs microdialysis sampling.<sup>32,36-41</sup> Emerging evidence suggests that retrodialysis of dexamethasone (DEX), a glucocorticoid anti-inflammatory steroid, is a simple yet effective

strategy for mitigating the probe penetration injury. Recent work on the microdialysis of dopamine in the rat striatum shows that DEX reduces ischemia, suppresses glial activation, protects neurons and neuronal terminals, prevents the formation of a glial barrier, and reinstates normal dopamine activity in the tissues surrounding microdialysis probes.<sup>32–36</sup>

Here, we report that DEX offers similar benefits to the microdialysis of SD-induced glucose and  $K^+$  transients in the rat cortex. We inserted microdialysis probes, with and without DEX, into the cortex of rats and monitored SD-induced glucose and  $K^+$  transients 2 hrs, 5 days, or 10 days later. Retrodialysis of DEX improved the detection of SD-associated transients at all three time points. In our 10-day studies, DEX retrodialysis was performed only during the first 5 days, confirming that continuous DEX delivery for the entire 10-day time window is not required. Finally, histochemical analyses show that retrodialysis of DEX for 5 days prevented ischemia and gliosis at the tracks of probes implanted for 10 days. Our findings confirm that DEX enhances the performance of microdialysis for monitoring SD-induced glucose and  $K^+$  transients in the rat cortex for at least 10 days after probe insertion.

## RESULTS AND DISCUSSION

### Experimental Design.

Microdialysis probes were inserted into the rat cortex and used to monitor  $K^+$  and glucose in response to SD triggered by needle pricks 2 hrs, 5 days, or 10 days later. Due to the design of the experiments, different animals were used at each time point. For observations at 2 hrs after probe insertion, the animals were anesthetized for probe insertion and remained anesthetized for the duration of the experiment. For observations at 5 and 10 days after probe insertion, the animals were anesthetized for probe insertion, allowed to recover from anesthesia, housed in a Ratan system, and then re-anesthetized for the measurements. The anesthetic was isoflurane. Once inserted, all probes were perfused continuously at 1.67  $\mu\text{L}/\text{min}$ , with only occasional brief interruptions to refill the perfusion syringe. The probes were perfused with artificial cerebrospinal fluid (aCSF) either with or without DEX. For DEX retrodialysis, the concentration of DEX was 10  $\mu\text{M}$  for the first day of perfusion, 2  $\mu\text{M}$  for days 1–5, and zero for days 5–10.<sup>32,36</sup> For observations 10 days after probe insertion, the perfusion fluid was switched from DEX to aCSF on day 5.

Glucose and  $K^+$  were monitored with rsMD and an on-line ISE, respectively, as previously described (Figure 1).<sup>25</sup> *In vitro* probe recovery was  $64.0 \pm 1.5\%$  for  $K^+$  and  $10.1 \pm 0.6\%$  for glucose (mean  $\pm$  S.E.). The higher recovery for  $K^+$  is due to its small size compared to glucose. Probe recovery was constant when probes were stored in aCSF for 10 days (Table S1). Dialysate concentrations reported herein have not been corrected for probe recovery.

### Probe Insertion and Representative Observations.

Figure 2 shows an example of a complete recording of  $K^+$  and glucose from an acute experiment in a single rat. Prior to probe insertion the dialysate  $K^+$  and glucose concentrations, 2.7 mM and zero, respectively, derive from the perfusion fluid. In Figure 2 and all subsequent figures the  $K^+$  and glucose traces are time-adjusted according to  $t_1$  and  $t_2$  (see Figure 1) so that the transients are aligned in time with each other and with the needle

pricks. The vertical black lines mark the times at which the needle pricks were performed. The delay time between the needle pricks and the time-adjusted  $K^+$  transients, which begin at  $t_0$  (Figure 1), were typically less than 1 min. Each needle prick induced a clear  $K^+$  spike and a clear glucose dip, hallmarks of SD. The glucose dip is indicative of the energy consumed as the tissue repolarizes after SD.

A prominent  $K^+$  spike also occurred just after the microdialysis probe was inserted into the cortex (Figure 2). A few moments later, the glucose signal, which had been initially increasing towards a basal level, also dipped. This initial  $K^+$  spike and glucose dip, which indicate that probe insertion induces SD, were observed in all animals regardless of whether or not the perfusion fluid contained DEX (Figure 3). This insertion SD supports prior conclusions that probe insertion causes a penetration injury.<sup>28–41</sup>

In the case of Figure 2, after the insertion SD the dialysate glucose concentration increased quickly at first, stabilized, and then increased slowly but continuously until the needle pricks began. All animals exhibited some combination of drift and noise in the glucose baseline but there were no consistent trends between animals prior to the needle pricks. Inducing 3 consecutive needle pricks created a constant decline in the basal glucose in 65% of the animals studied (see Figure S1 for an example). This agrees with previous studies that showed when multiple SD events are clustered together it results in a decrease in basal glucose.<sup>18,20</sup>

Two additional examples of complete recordings of  $K^+$  and glucose from single animals are provided in the Supplementary Information. Figure S1 is an example with needle pricks that produced neither a  $K^+$  spike nor a glucose dip. Of the 104 needle pricks performed during this work, only 11 (~11%) produced neither a  $K^+$  spike nor a glucose dip. We assume that the needle prick either did not induce SD or that SD did not reach the location of the microdialysis probe. When this occurred, extra pricks were performed so that three SD responses were recorded from each animal.

Figure S2 shows a unique adverse event: in this one animal, the needle prick induced a long-lasting elevation in  $K^+$  and a long-lasting decline in glucose. The rat died about 1 hr later. This unique event resembles a phenomenon called spreading ischemia,<sup>42</sup> although without direct measurement of blood flow this cannot be confirmed.

### **SD-induced Transients 2 hours after Probe Insertion.**

Three needle pricks were performed at 30-min intervals beginning 2 hrs after insertion of microdialysis probes into the rat cortex. DEX increased the amplitudes of the SD-induced  $K^+$  spikes and glucose dips by 127% and 86% (averages of the three responses), respectively, compared to those observed without DEX (Figure 4: DEX also significantly increased the areas-under-the-curves, see Figure S3). The amplitudes of the  $K^+$  spikes and the glucose dips consistently decreased upon each consecutive needle prick (Figure 4) but this trend did not reach statistical significance (see the figure legend for the ANOVA details). We speculate this decreasing trend is a consequence of repetitively pricking the same cortical location.

### SD-induced Transients 5 days after Probe Insertion.

Probes were inserted and perfused with aCSF or DEX for 5 days. Then, rats were re-anesthetized 1 hr before the first needle prick. If a needle prick produced neither a K<sup>+</sup> spike nor a glucose dip, an extra needle prick was performed, as explained above. In some cases, however, the needle prick produced a K<sup>+</sup> spike but no detectable glucose dip (11 of 15 with aCSF and 3 of 15 with DEX). Such needle pricks were not repeated: instead, the glucose dip was rated as non-detectable. All needle pricks that induced a K<sup>+</sup> spike were included in the data analysis explained below.

Glucose dips were rated as non-detectable if their amplitude did not exceed 3x the baseline noise. The baseline noise was determined from the standard deviation of the glucose concentrations measured over the 10-min interval prior to each needle prick (Figure S4). By this procedure, the average glucose detection limit for the five groups in this study was  $37 \pm 16 \mu\text{M}$  (mean  $\pm$  S.E.): this value exceeds the rsMD detection limit of 25  $\mu\text{M}$  reported previously.<sup>43</sup> Thus, the limit of detection in this work is determined by the noise in the glucose baseline rather than the noise in the rsMD detector.

After microdialysis probes were perfused with aCSF for 5 days, the K<sup>+</sup> spikes were of low amplitude and the glucose dips were essentially non-detectable (Figure 5a). Fifteen K<sup>+</sup> spikes were observed (5 animals, 3 responses each) but only 4 were accompanied by glucose dips with amplitudes greater than 3x the baseline noise. As observed at 2 hrs, the amplitude of the consecutive K<sup>+</sup> spikes decreased upon each consecutive needle prick (Figure 5c), presumably due to repetitively pricking the same cortical location. Previously we showed that microdialysis probes are completely engulfed in a glial barrier 5 days after insertion,<sup>32,36</sup> thus we attribute the low amplitudes of these K<sup>+</sup> and glucose transients to the presence of the glial barrier.

After microdialysis probes were perfused with DEX for 5 days, needle pricks induced robust K<sup>+</sup> spikes and glucose dips (Figure 5b). We observed fifteen K<sup>+</sup> spikes and 12 (80%) of these were accompanied by quantifiable glucose dips. Averaging over the 3 consecutive needle pricks, the amplitudes of K<sup>+</sup> spikes measured with DEX were 184% larger than those measured without DEX (Figure 5c). The effect of DEX was significant (ANOVA details in the legend of Figure 5: statistical analysis of the glucose responses were not possible because those measured without DEX were not quantifiable, see Figure 5D). Previous studies show that DEX prevents the formation of a glial barrier at 5 day after probe insertion,<sup>32–36</sup> thus we attribute the enhanced detection of these K<sup>+</sup> and glucose transients to the absence of a glial barrier (see also Figure 8, below).

### SD-associated Transients 10 days after Probe Insertion.

Microdialysis probes were inserted into the rat cortex and responses to needle pricks were recorded 10 days later. DEX retrodialysis was performed only during the first 5 days. On the fifth day the perfusion fluid was switched from DEX to aCSF, which was perfused through the probes for the remainder of the experiments. There were two principal reasons for adopting this protocol. First, DEX is an exogenous agent. In most instances, whether working in animals or patients, it is preferable to use a minimum sufficient quantity of such

an exogenous agent. Second, prior work on neuroprosthetic devices suggests that continuous delivery of DEX might not be necessary for long-term benefits.<sup>44–46</sup>

Needle pricks performed 10 days after probe insertion induced robust K<sup>+</sup> spikes and corresponding glucose dips (Figure 6): 87% of the fifteen K<sup>+</sup> spikes were accompanied by a quantifiable glucose dip (Table 1). As observed at 2 hrs and 5 days, there was a decreasing trend in the amplitude of the K<sup>+</sup> spikes on each consecutive needle prick. However, no such trend appeared in the glucose responses, which exhibited consistent amplitudes. Figure 6 confirms the benefits of DEX retrodialysis for monitoring SD-induced K<sup>+</sup> and glucose transients outlast the duration of the DEX retrodialysis itself. Figure 6 is our first report of DEX-enhanced microdialysis at 10 days after probe insertion. Previously, we showed that 5 days of DEX retrodialysis reinstated normal dopamine neurochemical activity near the probe.<sup>36</sup> Here we extend that work not only to 10 days after probe insertion, a clinically relevant time window, but also to include the enhancement of monitoring K<sup>+</sup> and glucose transients in the context of SD.

### Quantitative Comparisons.

In the presence of DEX, the amplitudes of the K<sup>+</sup> spikes were significantly larger at 2 hrs compared to 5 and 10 days (Figure 7a). In contrast, there were no significant differences between the amplitudes of the glucose dips at the three time points (Figure 7b). In the presence of DEX, the fraction of K<sup>+</sup> spikes accompanied by quantifiable glucose dips was relatively constant across the three time points (Table 1). In the absence of DEX, glucose dips were essentially non-detectable 5 days after probe insertion (Table 1).

Prior to the start of the needle pricks the basal K<sup>+</sup> and glucose concentrations were  $3.1 \pm 0.1$  mM and  $374 \pm 36$   $\mu$ M, respectively (mean  $\pm$  S.E.,  $n = 31$  animals). There were no significant differences between the basal levels of the 5 groups analyzed in this study (one-way ANOVAs). This confirms that none of the probes failed during this study, including those perfused for 5 days without DEX.

### Immunohistochemistry.

We used fluorescence microscopy to examine thin sagittal sections of brain tissue containing the tracks of probes implanted for 10 days. Non-implanted control tissues from the contralateral hemisphere were used for comparison. When probes were perfused with DEX for 5 days after probe insertion, immunohistochemistry showed no evidence of ischemia (lack of nanobeads) or gliosis (GFAP) 10 days after probe insertion (Figure 8). When the percent of fluorescent pixels in images of probe tracks were compared to images of non-implanted control tissue, there were no significant differences between either the blood flow or gliosis images (Figure 8f: during the analysis the probe tracks themselves were excluded from the regions of interest). Figure 8 extends our previous reports that DEX prevents ischemia and gliosis.<sup>32–33</sup>

Figure 8 is our first report that DEX prevents ischemia and gliosis near probes inserted into the rat cortex, that the benefits of DEX last for 10 days after insertion, and that the benefits of DEX retrodialysis long outlast the DEX retrodialysis itself.

## CONCLUSIONS

Our findings confirm that DEX retrodialysis enhances the microdialysis detection of SD-induced  $K^+$  and glucose transients for at least 10 days after probe insertion. We observed an insertion SD (Figures 2 and 3), supplementing prior evidence that insertion causes a penetration injury.<sup>28–41</sup> Despite the penetration injury, brain microdialysis is well tolerated by animals and human patients alike, presumably because only a small volume of tissue is affected. The issue at hand, however, is the impact of the penetration injury-induced ischemia, cell loss, gliosis, and glial barrier formation on the outcome of brain microdialysis procedures.<sup>28–36</sup> Thus, our objective is to promote the recovery of normal brain function and activity at the probe site. Retrodialysis of DEX is emerging as simple yet effective strategy for achieving this objective.

Without DEX, SD-induced transients became difficult to monitor 5 days after probe insertion.  $K^+$  transients exhibited a significant decrease in amplitude and glucose transients became too small reliably quantify: 11 of 15 detected  $K^+$  spikes were not accompanied by any detectable glucose dip. These observations are consistent with the idea that the glial barrier prevents SD-induced transient detection by microdialysis.

With the retrodialysis of DEX, SD-induced  $K^+$  and glucose transients were reliably quantified 2 hrs, 5 days, and 10 days after probe insertion (Figures 4–6). This work is our first extension of DEX enhanced microdialysis to  $K^+$  and glucose transients, to the rat cortex, and to 10 days after probe insertion. We attribute the enhanced transient detection to DEX's ability to prevent ischemia, cell loss, gliosis, and glial barrier formation at the probe site. A key finding of the present study is that the beneficial effects of DEX persisted to 10 days after probe insertion even though we stopped retrodialysis of DEX on day 5.

With the retrodialysis of DEX, however, the amplitude of the  $K^+$  transients decreased systematically day-to-day (Figure 7). First, the amplitudes decreased in response to each consecutive needle prick: as mentioned above, this is likely because we repetitively pricked the same cortical location. Second, there was a statistically significant decrease from 2 hr to 5 days: however, there was no further significant decrease from 5 to 10 days. The amplitude of the glucose transients exhibited similar declining trends but these were not statistically significant (Figure 7). Overall, these day-to-day declines might be an indication that the tissue next to the probe becomes more tolerant of SD over time. Brain tissue depends on the vasculature for moment-to-moment delivery of glucose and oxygen to meet the energy demands of re-polarization after SD.<sup>7</sup> Retrodialysis with DEX reinstates blood flow to the probe track at 5 days following insertion<sup>32</sup> and Figure 8 documents that this persists to 10 days. We speculate, therefore, that the declining response amplitudes, especially of the  $K^+$  transients, reflect an improvement in the health status of the tissue at the probe track.

Furthermore, we found no evidence of inherent probe failure during this work. During a 10-day in vitro test, recovery for  $K^+$  and glucose remained constant (Table S1). During in vivo procedures, all probes maintained consistent flow without evidence of clogging, increased flow resistance, or other flow problems. Moreover, there were no statistically significant differences among the basal glucose and  $K^+$  levels, measured just prior to the onset of the

needle prick procedures, regardless of post-insertion time or inclusion of DEX. All probes, regardless of conditions, reported a basal dialysate glucose level near 375  $\mu\text{M}$  and  $\text{K}^+$  near 3.1 mM. For this reason, we conclude that the key factor determining the ability to detect SD-induced transients by microdialysis is the status of the tissue adjacent to the probe: the probes themselves show no signs of failure over the course of our 10-day studies.

Although this work was conducted in animals, our eventual goal is clinical translation. We hypothesize that the combination of rsMD with DEX-enhanced microdialysis has the potential to impact clinical microdialysis in important ways. Traditional clinical microdialysis has been previously performed in TBI patients for 10 days with a microdialysis sampling time of 1 hr and without DEX or any other strategy to mitigate the consequences of the probe insertion.<sup>22–23</sup> A correlation was found between dialysate glucose levels during the first 50 hrs of microdialysis and patient outcome.<sup>22</sup> However, no correlation was found 2–10 days after probe insertion. This latter observation is perplexing, because ECoG detects SD in TBI patients well beyond 50 hrs.<sup>11,14,17,18</sup> Although it remains to be seen, we are hopeful that the combination of rsMD with DEX retrodialysis will offer enhanced microdialysis monitoring capabilities for patients at risk of secondary injury by SD.

## METHODS

All procedures involving animals were approved by the University of Pittsburgh Institutional Animal Care and Use Committee.

### Reagents and Solutions.

All solutions were prepared with ultrapure water (Nanopure; Barnstead, Dubuque, IA). Artificial cerebrospinal fluid (aCSF) contained 142 mM NaCl, 1.2 mM  $\text{CaCl}_2$ , 2.7 mM KCl, 1.0 mM  $\text{MgCl}_2$ , and 2.0 mM  $\text{NaH}_2\text{PO}_4$ , adjusted to a pH 7.4. Dexamethasone sodium phosphate (APP Fresenius Kabi USA, LLC, Lake Zurich IL) was diluted in aCSF. The microdialysis perfusion fluids were filtered with Nalgene sterile filter units (Fisher, Pittsburgh, PA; PES 0.2  $\mu\text{m}$  pores). Glucose oxidase (GOx, 100–200 units/mg) and horseradish peroxidase (HRP, 250 units/mg) were obtained from Sigma Aldrich. The ferrocene solution contained 1.5 mM ferrocenecarboxylic acid, 1 mM EDTA, 150 mM sodium chloride and 100 mM sodium citrate and was filtered before use with 0.1  $\mu\text{m}$  and 0.02  $\mu\text{m}$  pore size filters.

### Microdialysis Probes, Surgical Procedures, and Experiment Protocol.

Concentric style microdialysis probes were built in-house with hollow fiber membranes (13 kD MWCO, Specta/Por RC, Spectrum, Ranco Dominguez, CA), 4 mm in length and 280  $\mu\text{m}$  in outer diameter. Fused silica capillaries (75  $\mu\text{m}$  I.D., 150  $\mu\text{m}$  O.D., Polymicro Technologies, Phoenix, AZ) were used for the inlet and outlet lines. Prior to use, probes were soaked in 70% ethanol and then flushed and immersed in aCSF (or aCSF with DEX) for several hrs prior to implantation into the brain. Prior to insertion, the probe inlet was connected to a 1 mL gas tight syringe driven by a microliter syringe pump (Harvard



Apparatus, Holliston, MA) at a perfusion rate of 1.67  $\mu\text{L}/\text{min}$ . The probe outlet (50 cm long) was connected to the  $\text{K}^+$  ISE detector.

Rats (male, Sprague-Dawley, 250–350g, Charles River, Raleigh, NC) were anesthetized with isoflurane (5% induction, 2.5% maintenance), placed in a stereotaxic frame (David Kopf Instruments, Tujunga, CA, USA) and adjusted to flat skull<sup>47</sup> for probe insertion. Aseptic technique was used throughout. The microdialysis probe was lowered at a 51° angle into the cortex using the coordinates 4.2 mm posterior to bregma, 1.5 mm lateral to midline, and 4 mm below dura: the entire active portion of the probe came to rest in the cortex. For the 2-hr study, the rats (n=8 per group) remained under anesthesia for the duration of the experiment and responses to needle pricks were monitored beginning 2 hrs after probe insertion. To perform the needle pricks, a second hole was drilled through the skull ipsilateral to the probe, just anterior to bregma (approximately 4.5 mm from the probe). The surface of the cortex was manually pricked with the tip of an 18-gauge hypodermic needle. Three pricks, 30 min apart, were performed per animal. For the 5- and 10-day experiments (n=5 per group), the probes were inserted as described above and secured with bone screws and acrylic cement. The incision was closed with sutures, anesthesia was removed, and the rats were housed in a Ratur Microdialysis Bowl (MD-1404, BASI, West Lafayette, IN) with continuous perfusion of the microdialysis probe at 1.67 $\mu\text{L}/\text{min}$ . When used, the concentration of DEX was 10  $\mu\text{M}$  for the first 24 hrs and then 2  $\mu\text{M}$  for the next five days.<sup>32,36</sup> After 5 or 10 days the rats were re-anesthetized 1 hr prior to recording responses to needle pricks.

### Potassium and Glucose Detection.

The  $\text{K}^+$  ISE electrode and poly(dimethyl)siloxane (PDMS) microfluidic system have been described previously.<sup>24</sup> Briefly, a miniaturized  $\text{K}^+$  ISE was made in-house. A membrane containing 2 mg potassium ionophore, 0.2 mg potassium tetrakis(4-chlorophenyl)borate, 150.0 mg bis(2-ethylhexyl) sebacate, and 66 mg poly(vinyl chloride) (PVC) dissolved in tetrahydrofuran (reagents from Sigma-Aldrich) was cast over a segment of perfluoroalkoxyalkane tubing (PFA, IDEX Health Sciences, 360  $\mu\text{m}$  O.D. and 150  $\mu\text{m}$  I.D). The electrode was assembled with an internal Ag/AgCl reference and aCSF filling solution. The potential of the  $\text{K}^+$  ISE was measured against an external Ag/AgCl reference electrode using custom electronics built in-house. The  $\text{K}^+$  ISE and external reference electrode were inserted into a PDMS chip fabricated with soft lithography, as shown in Figure 1. The total internal volume of the PDMS chip is approximately 700 nL. Connections to and from the PDMS chip were made with 0.15 mm and 0.13 mm ID FEP tubing, respectively.

The rapid sampling microdialysis (rsMD) system has been described previously.<sup>19</sup> Briefly, the dialysate enters a custom built sampling valve (Valco, Switzerland) with two 100 nL internal sampling loops. A standard HPLC pump (flow rate: 200  $\mu\text{L}/\text{min}$ ) mixed ferrocene solution with the dialysate and injected the mixture at 30 second intervals into one of two paths, both of which contain dual enzyme reactors in-line with a 3 mm glassy carbon disk electrode. The enzyme reactor contained two 6 mm-diameter membranes (0.025  $\mu\text{m}$  pores, Millipore) loaded with glucose oxidase (1 mg/mL) or horseradish peroxidase (0.5 mg/mL).

The reduction of the ferrocenium ion was measured at 0 V with a three-electrode system with a Ag/AgCl reference electrode (UniJet, BASi, USA) and custom-built electronics.

### Data Analysis.

The rsMD data were analyzed with previously published algorithms<sup>43</sup> and converted to concentration with post-experiment calibrations. In Figures 2–6 the  $K^+$  and glucose recordings were time-aligned to  $t_0$  (Figure 1) to account for the travel time to and between the sensors. At the 1.67  $\mu\text{L}/\text{min}$  flow rate it takes approximately 4 mins,  $t_1$ , for the sample to travel to the  $K^+$  sensor and an additional 7 mins,  $t_2$ , to travel to the glucose detector (Figure 1). The  $K^+$  spikes were used to confirm SD at the probe site: if there was no  $K^+$  spike the needle prick was repeated (see discussion of Figure S1). A 10-min baseline prior to the expected glucose response was used to calculate a threshold for a detectable glucose signal, defined as 3x the noise of the 10 min baseline. If the glucose level dropped below the threshold in the next 15 minutes it was included as a detectable response (see Figure S4). Only detectable glucose responses were included in the data analysis and figures. A  $K^+$  threshold was calculated in a similar manner using the signal recorded for 2 mins prior to needle pricks.

### Immunohistochemistry and fluorescence microscopy.

The procedures for immunohistochemistry and fluorescence microscopy are described in our previous papers.<sup>32,48–49</sup> Rats were deeply anesthetized with isoflurane (2.5% by volume  $\text{O}_2$ ) and perfused transcardially with 200 ml 0.01 M phosphate-buffered saline (PBS), pH 7.4, followed by 160mL of 4% paraformaldehyde, and then with 50mL of a solution containing commercially available (Molecular Probes) 100-nm fluorescent beads (1:1000 dilution PBS). The entire brain was quickly removed and further fixed in 4% paraformaldehyde for 24 h at 4°C before being equilibrated in a 30% sucrose solution at 4°C for 24 hrs. The brain was then frozen in 2-methylbutane in a bath of liquid nitrogen to prevent freeze fracturing. The tissue containing the probe track was cut to 20- $\mu\text{m}$  sagittal sections ( $n=3$ , 3 slides per animal). Free floating sections were rinsed in PBS, three times (10 min each), then blocked with 5% goat serum in PBS containing 0.1% Triton X-100 for 1 h at room temperature and subjected to immunohistochemical staining. The sections were incubated overnight at 4°C with the primary antibody anti-glia fibrillary acidic protein (GFAP; 1:100; #Z033401, DAKO Agilent Technologies). As a negative control, PBS was used instead of the primary antibody. Sections were then washed with PBS (5 min) and incubated in a secondary solution consisting of 5% goat serum, 0.1% Triton X-100, and antibody (1:500 goat anti-rabbit Alexa 568, Invitrogen, Carlsbad CA) for 2 hrs at room temperature. Sections were then rinsed with PBS for 10 min before being cover slipped with Fluoromount-G (Southern Biotech, Birmingham AL). Sections were imaged using fluorescent microscopy (FluoView 1000, Olympus, Inc., Tokyo, Japan) at 20x magnification.

Tissue images were processed and analyzed with the Metamorph/Fluor 7.1 software package (Universal Imaging Corporation; Molecular Devices). Quantitative analysis was based on individual sections containing the microdialysis probe track in the ipsilateral region. Sections from the contralateral region (non-implanted control tissue) were treated in identical fashion to the ipsilateral region. The fluorescence intensities of GFAP and blood

flow were determined by setting threshold values; the total number of pixels was expressed as the percent of fluorescence in the region of interest.<sup>33</sup> Samples were compared to a non-implanted region of the tissue slice.

### Statistics.

IBM Statistical Package for the Social Sciences (SPSS) 22 software was used for all statistical analysis. For all tests a  $p < 0.05$  was used for statistical significance.

### Supplementary Material

Refer to Web version on PubMed Central for supplementary material.

### Acknowledgments

#### Funding

This work was funded by the NIH (NS092245), NSF Graduate Research Fellowship Program (ELV, 1247842), and University of Pittsburgh's Center for Biologic Imaging (1S10RR028478-01: for the use of the Olympus FluoView 1000)

### ABBREVIATIONS

<b>SD</b>	Spreading Depolarization
<b>TBI</b>	traumatic brain injury
<b>DEX</b>	dexamethasone
<b>aCSF</b>	artificial cerebrospinal fluid
<b>ISE</b>	ion selective electrode
<b>rsMD</b>	rapid sampling microdialysis
<b>PDMS</b>	poly(dimethyl)siloxane
<b>ANOVA</b>	analysis of variance
<b>GFAP</b>	glial fibrillary acidic protein
<b>PBS</b>	phosphate-buffered saline

### REFERENCES.

- 1). Langlois JA, Rutland-Brown W, and Wald MM (2006) The epidemiology and impact of traumatic brain injury: a brief overview, *J Head Trauma Rehabil*, 21, 375–378. [PubMed: 16983222]
- 2). “Traumatic brain injury: time to end the silence”, (2010) *The Lancet Neurology* 9, 331. [PubMed: 20298955]
- 3). Faul M XL, Wald MM, Conrodado V (2010) Traumatic brain injury in the United States: Emergency Department Visits, Hospitalizations and Deaths 2002–2006, Atlanta (GA): Centers for Disease Control and Prevention, National Center for Injury Prevention and Control.
- 4). Leao AAP (1944) Spreading depression of activity in the cerebral cortex, *J Neurophysiol*, 7, 359–390.

- 5). Leao AAP (1947) Further observations of the spreading depression of activity in the cerebral cortex, *J Neurophysiol*, 10, 409–414. [PubMed: 20268874]
- 6). Strong AJ, Fabricius M, Boutelle MG, Hibbins SJ, Hopwood SE, Jones R, Parkin MC, and Lauritzen M (2002) Spreading and synchronous depressions of cortical activity in acutely injured human brain, *Stroke* 33, 2738–2743. [PubMed: 12468763]
- 7). Ayata C, and Lauritzen M (2015) Spreading Depression, Spreading Depolarizations, and the Cerebral Vasculature, *Physiol. Rev*, 95, 953–993. [PubMed: 26133935]
- 8). Dreier JP (2011) The role of spreading depression, spreading depolarization and spreading ischemia in neurological disease, *Nat. Med*, 17, 439–447. [PubMed: 21475241]
- 9). Dreier JP, et al. (2016) Recording, analysis, and interpretation of spreading depolarizations in neurointensive care: Review and recommendations of the COSBID research group, *J Cereb Blood Flow Metab* Epub ahead of print.
- 10). Lauritzen M, Dreier JP, Fabricius M, Hartings JA, Graf R, and Strong AJ (2011) Clinical relevance of cortical spreading depression in neurological disorders: migraine, malignant stroke, subarachnoid and intracranial hemorrhage, and traumatic brain injury, *J Cereb Blood Flow Metab*, 31, 17–35. [PubMed: 21045864]
- 11). Hartings JA, Bullock MR, Okonkwo DO, Murray LS, Murray GD, Fabricius M, Maas AI, Woitzik J, Sakowitz O, Mathern B, Roozenbeek B, Lingsma H, Dreier JP, Puccio AM, Shutter LA, Pahl C, and Strong AJ (2011) Spreading depolarisations and outcome after traumatic brain injury: a prospective observational study, *Lancet Neurol*, 10, 1058–1064. [PubMed: 22056157]
- 12). Hartings JA, Watanabe T, Bullock MR, Okonkwo DO, Fabricius M, Woitzik J, Dreier JP, Puccio A, Shutter LA, Pahl C, and Strong AJ (2011) Spreading depolarizations have prolonged direct current shifts and are associated with poor outcome in brain trauma, *Brain*, 134, 1529. [PubMed: 21478187]
- 13). Hartings JA, Strong AJ, Fabricius M, Manning A, Bhatia R, Dreier JP, Mazzeo AT, Tortella FC, and Bullock MR (2009) Spreading depolarizations and late secondary insults after traumatic brain injury, *J. Neurotrauma*, 26, 1857–1866. [PubMed: 19508156]
- 14). Hinzman JM, Andaluz N, Shutter LA, Okonkwo DO, Pahl C, Strong AJ, Dreier JP, and Hartings JA (2014) Inverse neurovascular coupling to cortical spreading depolarizations in severe brain trauma, *Brain*, 137, 2960. [PubMed: 25154387]
- 15). Nakamura H, Strong AJ, Dohmen C, Sakowitz OW, Vollmar S, Sué M, Kracht L, Hashemi P, Bhatia R, Yoshimine T, Dreier JP, Dunn AK, and Graf R (2010) Spreading depolarizations cycle around and enlarge focal ischaemic brain lesions, *Brain*, 133, 1994. [PubMed: 20504874]
- 16). Dreier JP, Woitzik J, Fabricius M, Bhatia R, Major S, Drenckhahn C, Lehmann TN, Sarrafzadeh A, Willumsen L, Hartings JA, Sakowitz OW, Seemann JH, Thieme A, Lauritzen M, and Strong AJ (2006) Delayed ischaemic neurological deficits after subarachnoid haemorrhage are associated with clusters of spreading depolarizations, *Brain*, 129, 3224–3237. [PubMed: 17067993]
- 17). Fabricius M, Fuhr S, Bhatia R, Boutelle M, Hashemi P, Strong AJ, and Lauritzen M (2006) Cortical spreading depression and peri-infarct depolarization in acutely injured human cerebral cortex, *Brain*, 129, 778–790. [PubMed: 16364954]
- 18). Feuerstein D, Manning A, Hashemi P, Bhatia R, Fabricius M, Tolia C, Pahl C, Ervine M, Strong AJ, and Boutelle MG (2010) Dynamic metabolic response to multiple spreading depolarizations in patients with acute brain injury: an online microdialysis study, *J. Cereb. Blood Flow Metab*, 30, 1343–1355. [PubMed: 20145653]
- 19). Jones DA, Parkin MC, Langemann H, Landolt H, Hopwood SE, Strong AJ, and Boutelle MG (2002) On-line monitoring in neurointensive care: Enzyme-based electrochemical assay for simultaneous, continuous monitoring of glucose and lactate from critical care patients, *J. Electroanal. Chem*, 538–539, 243–252.
- 20). Parkin M, Hopwood S, Jones DA, Hashemi P, Landolt H, Fabricius M, Lauritzen M, Boutelle MG, and Strong AJ (2005) Dynamic changes in brain glucose and lactate in pericontusional areas of the human cerebral cortex, monitored with rapid sampling on-line microdialysis: relationship with depolarisation-like events, *J. Cereb. Blood Flow Metab*, 25, 402–413. [PubMed: 15703701]

- 21). Rogers ML, Leong CL, Gowers SA, Samper IC, Jewell SL, Khan A, McCarthy L, Pahl C, Toliaas CM, Walsh DC, Strong AJ, and Boutelle MG (2016) Simultaneous monitoring of potassium, glucose and lactate during spreading depolarisation in the injured human brain - Proof of principle of a novel real-time neurochemical analysis system, continuous online microdialysis, *J. Cereb. Blood Flow Metab* Epub ahead of print.
- 22). Vespa PM, McArthur D, O'Phelan K, Glenn T, Etchepare M, Kelly D, Bergsneider M, Martin NA, and Hovda DA (2003) Persistently low extracellular glucose correlates with poor outcome 6 months after human traumatic brain injury despite a lack of increased lactate: a microdialysis study, *J. Cereb. Blood Flow Metab*, 23, 865–877. [PubMed: 12843790]
- 23). Vespa P, Bergsneider M, Hattori N, Wu H-M, Huang S-C, Martin NA, Glenn TC, McArthur DL, and Hovda DA (2005) Metabolic crisis without brain ischemia is common after traumatic brain injury: a combined microdialysis and positron emission tomography study, *J. Cereb. Blood Flow Metab*, 25, 763–774. [PubMed: 15716852]
- 24). Papadimitriou KI, Wang C, Rogers ML, Gowers SA, Leong CL, Boutelle MG, and Drakakis EM (2016) High-Performance Bioinstrumentation for Real-Time Neuroelectrochemical Traumatic Brain Injury Monitoring, *Front. Hum. Neurosci*, 10, 212. [PubMed: 27242477]
- 25). Rogers ML, Feuerstein D, Leong CL, Takagaki M, Niu X, Graf R, and Boutelle MG (2013) Continuous Online Microdialysis Using Microfluidic Sensors: Dynamic Neurometabolic Changes during Spreading Depolarization, *ACS Chem. Neurosci*, 4, 799–807. [PubMed: 23574576]
- 26). Watson CJ, Venton BJ, and Kennedy RT (2006) In Vivo Measurements of Neurotransmitters by Microdialysis Sampling, *Anal. Chem*, 78, 1391–1399. [PubMed: 16570388]
- 27). Westerink BH, Cremers TIFH, Eds. (2007) *Handbook of Microdialysis: Methods, Applications, and Perspectives*, Academic Press, London.
- 28). Benveniste H, and Diemer NH (1987) Cellular reactions to implantation of a microdialysis tube in the rat hippocampus, *Acta Neuropathol*, 74, 234–238. [PubMed: 3673515]
- 29). Clapp-Lilly KL, Roberts RC, Duffy LK, Irons KP, Hu Y, and Drew KL (1999) An ultrastructural analysis of tissue surrounding a microdialysis probe, *J Neurosci. Methods*, 90, 129–142. [PubMed: 10513596]
- 30). Hascup ER, af Bjerken S, Hascup KN, Pomerleau F, Huettl P, Stromberg I, and Gerhardt GA (2009) Histological studies of the effects of chronic implantation of ceramic-based microelectrode arrays and microdialysis probes in rat prefrontal cortex, *Brain Res*, 1291, 12–20. [PubMed: 19577548]
- 31). Zhou F, Zhu X, Castellani RJ, Stimmelmayer R, Perry G, Smith MA, and Drew KL (2001) Hibernation, a model of neuroprotection, *Am. J. Pathol*, 158, 2145–2151. [PubMed: 11395392]
- 32). Jaquins-Gerstl A, Shu Z, Zhang J, Liu Y, Weber SG, and Michael AC (2011) Effect of dexamethasone on gliosis, ischemia, and dopamine extraction during microdialysis sampling in brain tissue, *Anal. Chem*, 83, 7662–7667. [PubMed: 21859125]
- 33). Nesbitt KM, Jaquins-Gerstl A, Skoda EM, Wipf P, and Michael AC (2013) Pharmacological Mitigation of Tissue Damage during Brain Microdialysis, *Anal. Chem*, 85, 8173–8179. [PubMed: 23927692]
- 34). Nesbitt KM, Varner EL, Jaquins-Gerstl A, and Michael AC (2015) Microdialysis in the Rat Striatum: Effects of 24 h Dexamethasone Retrodialysis on Evoked Dopamine Release and Penetration Injury, *ACS Chem. Neurosci*, 6, 163–173. [PubMed: 25491242]
- 35). Kozai TD, Jaquins-Gerstl AS, Vazquez AL, Michael AC, and Cui XT (2016) Dexamethasone retrodialysis attenuates microglial response to implanted probes in vivo, *Biomaterials*, 87, 157–169. [PubMed: 26923363]
- 36). Varner EL, Jaquins-Gerstl A, and Michael AC (2016) Enhanced Intracranial Microdialysis by Reduction of Traumatic Penetration Injury at the Probe Track, *ACS Chem. Neurosci*, 7, 728–736. [PubMed: 27003503]
- 37). Robinson TE, and Camp DM (1991) The effects of four days of continuous striatal microdialysis on indices of dopamine and serotonin neurotransmission in rats, *J. Neurosci. Methods*, 40, 211–222. [PubMed: 1724788]

- 38). Sharp T, Ljungberg T, Zetterstrom T, and Ungerstedt U (1986) Intracerebral dialysis coupled to a novel activity box--a method to monitor dopamine release during behaviour, *Pharmacol. Biochem. Behav*, 24, 1755–1759. [PubMed: 3737640]
- 39). Holson RR, Gazzara RA, and Gough B (1998) Declines in stimulated striatal dopamine release over the first 32 h following microdialysis probe insertion: generalization across releasing mechanisms, *Brain Res*, 808, 182–189. [PubMed: 9767162]
- 40). Holson RR, Bowyer JF, Clausing P, and Gough B (1996) Methamphetamine-stimulated striatal dopamine release declines rapidly over time following microdialysis probe insertion, *Brain Res*, 739, 301–307. [PubMed: 8955951]
- 41). Bungay PM, Newton-Vinson P, Isele W, Garris PA, and Justice JB (2003) Microdialysis of dopamine interpreted with quantitative model incorporating probe implantation trauma, *J. Neurochem*, 86, 932–946. [PubMed: 12887691]
- 42). Hartings JA, Shuttleworth CW, Kirov SA, Ayata C, Hinzman JM, Foreman B, Andrew RD, Boutelle MG, Brennan KC, Carlson AP, Dahlem MA, Drenckhahn C, Dohmen C, Fabricius M, Farkas E, Feuerstein D, Graf R, Helbok R, Lauritzen M, Major S, Oliveira-Ferreira AI, Richter F, Rosenthal ES, Sakowitz OW, Sanchez-Porras R, Santos E, Scholl M, Strong AJ, Urbach A, Westover MB, Winkler MK, Witte OW, Woitzik J, and Dreier JP (2016) The continuum of spreading depolarizations in acute cortical lesion development: Examining Leao's legacy, *J. Cereb. Blood Flow Metab*, In Press doi: 10.1177/0271678X16654495.
- 43). Feuerstein D, Parker KH, and Boutelle MG (2009) Practical Methods for Noise Removal: Applications to Spikes, Nonstationary Quasi-Periodic Noise, and Baseline Drift, *Anal. Chem* 81, 4987–4994. [PubMed: 19449858]
- 44). Groothuis J, Ramsey NF, Ramakers GM, and van der Plasse G (2014) Physiological challenges for intracortical electrodes, *Brain Stimul*, 7, 1–6. [PubMed: 23941984]
- 45). Spataro L, Dilgen J, Retterer S, Spence AJ, Isaacson M, Turner JN, and Shain W (2005) Dexamethasone treatment reduces astroglia responses to inserted neuroprosthetic devices in rat neocortex, *Exp. Neurol*, 194, 289–300. [PubMed: 16022859]
- 46). Zhong Y, and Bellamkonda RV (2007) Dexamethasone-coated neural probes elicit attenuated inflammatory response and neuronal loss compared to uncoated neural probes, *Brain Res*, 1148, 15–27. [PubMed: 17376408]
- 47). Paxinos G, Watson C (1998) *The Rat Brain in Stereotaxic Coordinates*, 4<sup>th</sup> Edn, Academic Press, San Diego, CA.<sup>th</sup>
- 48). Jaquins-Gerstl A, and Michael AC (2009) Comparison of the brain penetration injury associated with microdialysis and voltammetry, *J. Neurosci. Methods*, 183, 127–135. [PubMed: 19559724]
- 49). Mitala CM, Wang Y, Borland LM, Jung M, S, S, Watkins S, Weber SG, and Michael AC (2008) Impact of microdialysis probes on vasculature and dopamine in the rat striatum: a combined fluorescence and voltammetric study, *J. Neurosci. Methods*, 174, 177–185. [PubMed: 18674561]

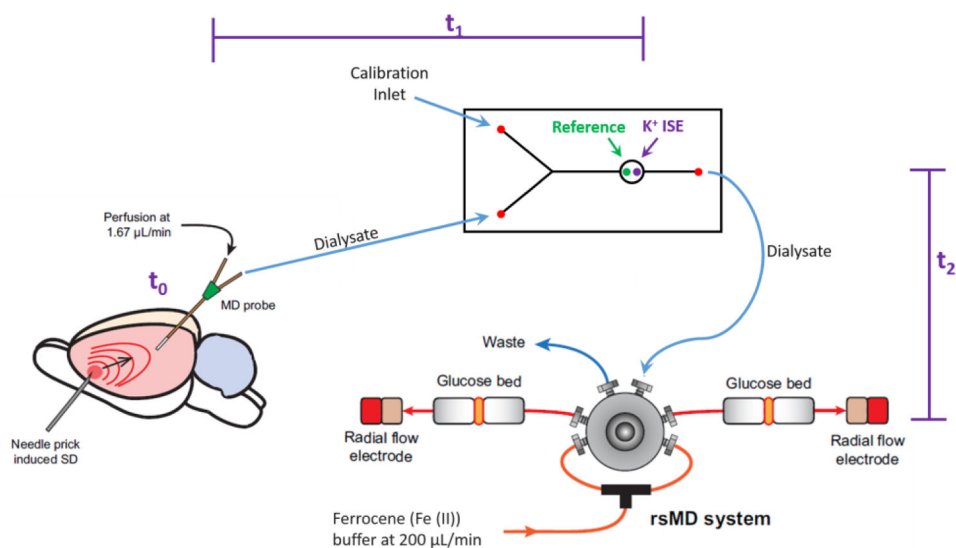


**Figure 1.** Experimental design. SD was induced by needle pricks in the cortex. The SD arrives at the microdialysis probe at  $t_0$ ; intervals between the needle pricks and  $t_0$  were typically less than 1 min. Next, the sample travels to the K<sup>+</sup> ISE in approximately 4 min,  $t_1$ . Finally, the sample travels to the glucose detector in approximately 7 min,  $t_2$ . Recordings of K<sup>+</sup> and glucose in Figures 2–6 are time-adjusted to account for  $t_1$  and  $t_2$ .

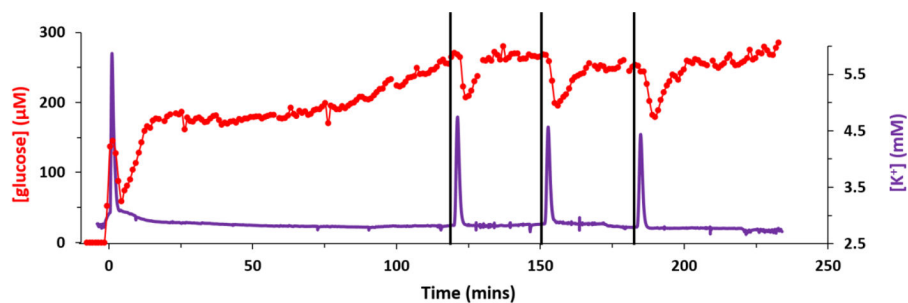


**Figure 2.**

A representative complete recording of  $K^+$  (purple) and glucose (red) from an acute experiment performed in one rat. The microdialysis probe was inserted at time 0 with DEX perfusion. Then, 2 hrs later, three needle pricks were performed 30 mins apart (black lines mark when the needle pricks occurred). The  $K^+$  and glucose traces have been time-adjusted to account for  $t_1$  and  $t_2$  (defined in Figure 1).



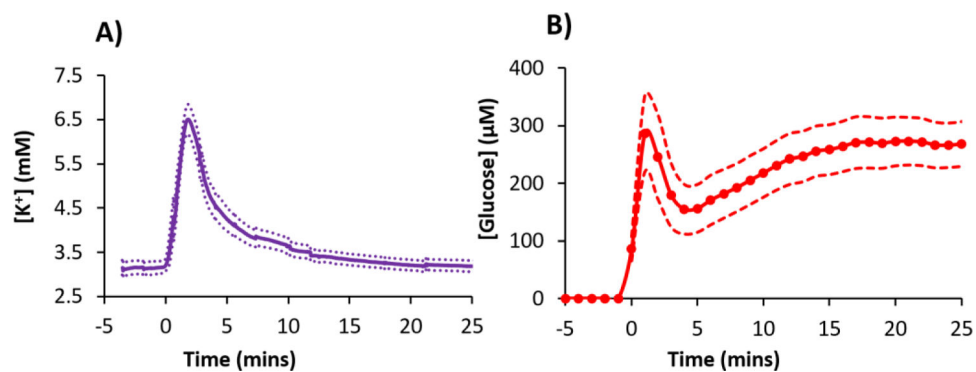


**Figure 3.** Probe insertion SD in the rat cortex characterized by A) an increase in  $K^+$  ( $K^+$  spike) and B) a decrease in glucose (glucose dip) time-aligned to the probe insertion at time zero (mean  $\pm$  SEM, n=16 rats). In this figure, t=0 is the time at which probe insertion was completed: note, however, that recovery of  $K^+$  and glucose begins as soon as the probe contacts brain tissue.

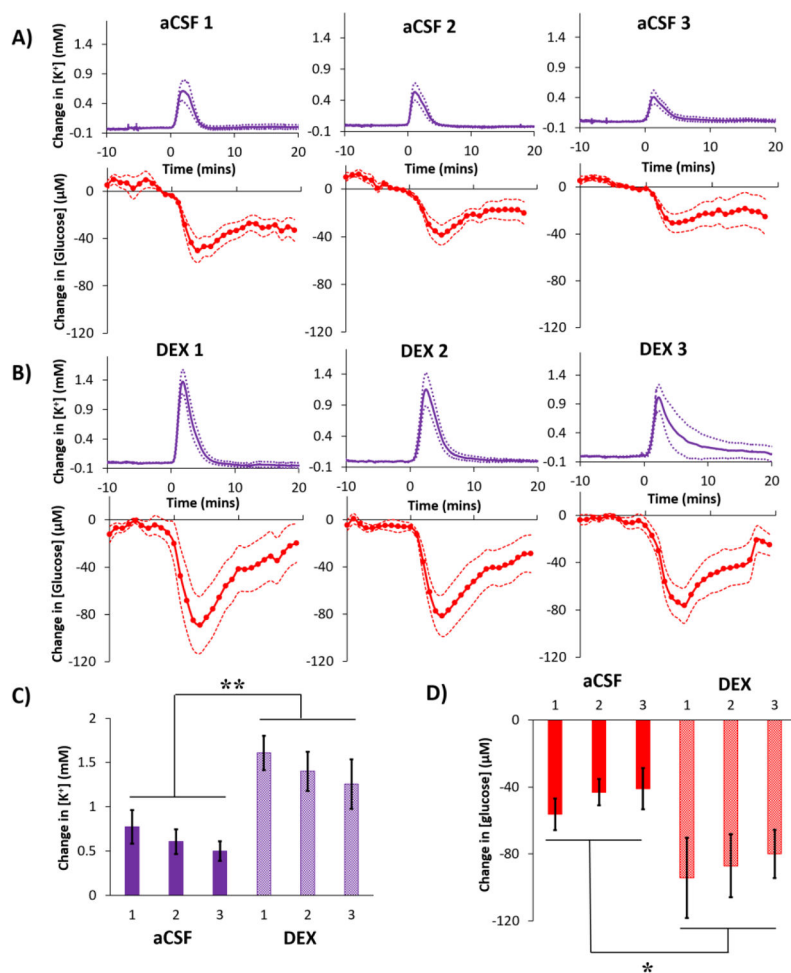


**Figure 4.** Cortical responses to 3 needle pricks recorded 2 hrs after probe insertion with A) aCSF or B) DEX (mean  $\pm$  SEM,  $n = 8$  rats (24 needle pricks) per group). Maximum changes in C) K<sup>+</sup> and D) glucose were analyzed with 2-way ANOVAs with group (aCSF, DEX) and needle prick (1,2,3; repeated measures) as the factors. The needle prick and interactions were not significant, but group was significant for both K<sup>+</sup> ( $F(1,14) = 13.422$ ) and glucose ( $F(1,14) = 6.253$ ). \*\* $p < 0.005$ , \* $p < 0.05$

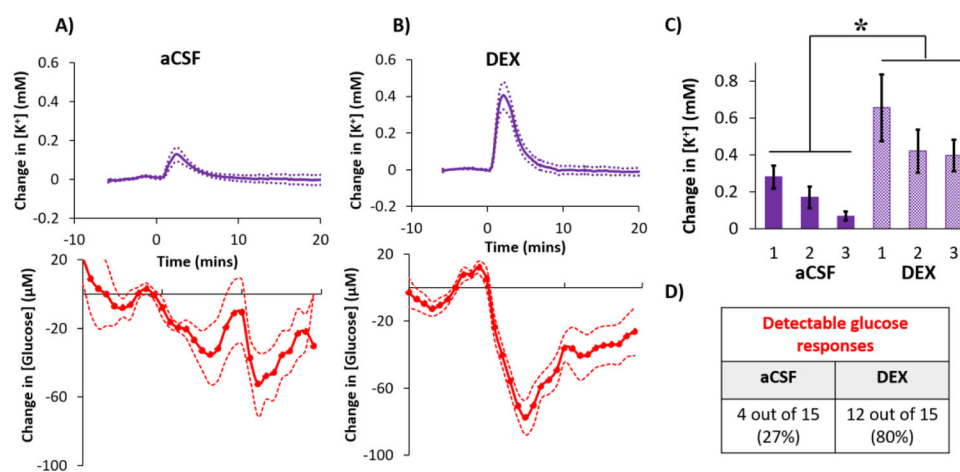


**Figure 5.** Average cortical response to needle pricks recorded 5 days after probe insertion with A) aCSF or B) DEX (mean  $\pm$  SEM,  $n = 5$  rats (15 needle pricks) per group). C) Changes in  $K^+$  to the 3 needle pricks were analyzed with a 2-way ANOVA with group (aCSF, DEX) and needle prick (1,2,3; repeated measures) as the factors. Group ( $F(1,8) = 5.844$ ,  $p < 0.05$ ) and needle prick ( $F(2,16) = 12.689$ ,  $p < 0.001$ ) are significant, interaction is not significant. D) Only detectable glucose responses are represented in A and B, see Table1 and S4 for details. \* $p < 0.05$ .

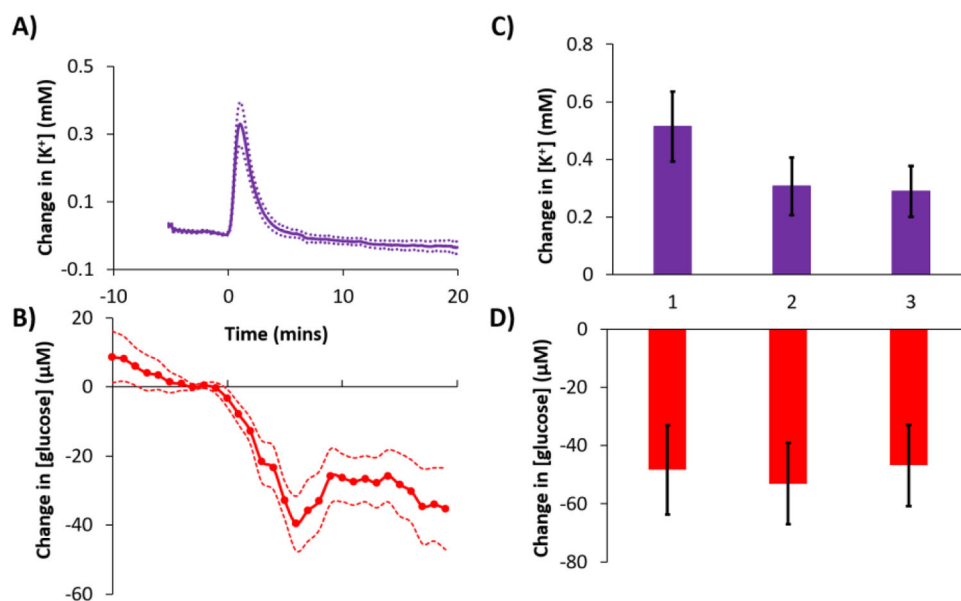


**Figure 6.**

A) K<sup>+</sup> and B) glucose response (mean ± SEM) to needle pricks performed 10 days after probe insertion (n=5 rats, 15 needle pricks). C and D provide the changes in K<sup>+</sup> and glucose, respectively, to each of the 3 needle pricks. Needle prick number was not a significant factor for either K<sup>+</sup> or glucose (1-way ANOVAs, repeated measures). The microdialysis probe was perfused with DEX for days 1–5 and then aCSF for days 5–10.

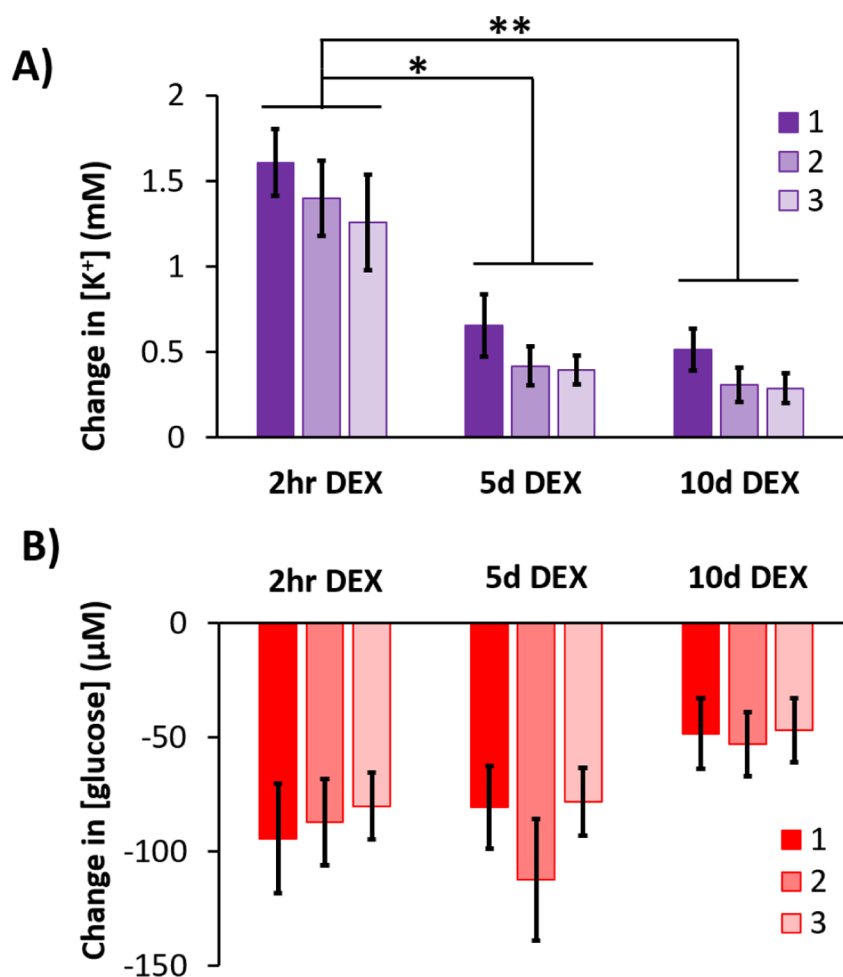


**Figure 7.** Summary comparison (mean  $\pm$  SEM) of the amplitudes of A) K<sup>+</sup> spikes and B) glucose dips in response to 3 needle pricks recorded 2 hrs, 5 days, and 10 days after probe insertion in the presence of DEX. Data were analyzed with a 2-way ANOVA with time (2 hr, 5 d, 10 d) and needle prick (1, 2, 3; repeated measures) as the factors. K<sup>+</sup>: time is significant ( $F(2,15)=15.878$ ,  $p < 0.0005$  while needle prick and the interaction are not significant. Glucose: neither factor was significant. Stars represent Games-Howell post-hoc tests, \*\* $p < 0.001$  and \* $p < 0.005$ .

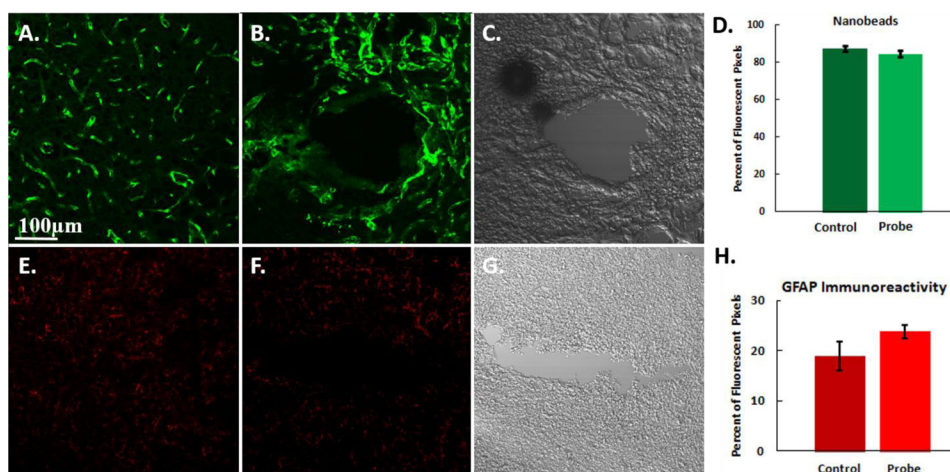


**Figure 8.** Representative fluorescent microscopy images of the probe tracks after 10 days. The cortex is labeled for A,B) blood flow (fluorescent nanobeads) and E,F) GFAP immunoreactivity. The left column (A,E) is control, non-implanted cortex tissue from the contralateral hemisphere. The center column (B,F) is tissue surrounding the microdialysis probe 10 days after probe implantation (5 days of DEX). The DIC images (C and G) are provided to identify the location of the microdialysis probe tracks in B and F. Graphs comparing the D) blood flow and H) GFAP immunoreactivity in the areas of interest in both the ipsilateral and contralateral hemispheres. There is no significant difference between probe tracks and control tissue for either nanobeads or GFAP (t-tests). Results are reported as the percent of fluorescent pixels (mean ± SEM). Scale bar is 100 μm.

**Table 1.**

Summary of the number of K<sup>+</sup> spikes and corresponding quantifiable glucose dips. Observation of a K<sup>+</sup> spike confirmed SD in the vicinity of the probe. In every case, except for 5d aCSF, the majority of the K<sup>+</sup> spikes were accompanied by a quantifiable glucose dip. Only the quantifiable glucose dips are included in Figures 4–7. The noise in a 10-min glucose baseline prior to each needle prick was used to create a threshold quantifiable glucose value (see text and Figure S4 for details).

	Total [K <sup>+</sup> ] transients	Quantifiable changes in [glucose]
<b>2hr DEX</b>	24	24 (100%)
<b>2hr aCSF</b>	24	21 (88%)
<b>5d DEX</b>	15	12 (80%)
<b>5d aCSF</b>	15	4 (27%)
<b>10d DEX</b>	15	13 (87%)

Author Manuscript

Author Manuscript

Author Manuscript

Author Manuscript